

## SOUR TOP OF THE LINE CORROSION IN THE PRESENCE OF ACETIC ACID

Singer M., Camacho A. \*, Brown B, Nestic S.  
Ohio University - Institute for Corrosion and Multiphase Technology  
342 West State St., Athens, OHIO, 45701  
e-mail: [singer@bobcat.ent.ohiou.edu](mailto:singer@bobcat.ent.ohiou.edu)

### ABSTRACT

Under stratified flow and dewing conditions, internal corrosion can occur at the top of horizontal pipelines where continuous injection of corrosion inhibitors does not have a mitigating effect. This research work presents an experimental study of the influence of the presence of H<sub>2</sub>S (up to 0.13 bars) and acetic acid (up to 1000 ppm) on the more standard CO<sub>2</sub> Top of the Line Corrosion. A comprehensive analysis on the effect of these parameters on the type of corrosion product film formed at the top of the line is performed.

**Key Words:** Top of the line corrosion, H<sub>2</sub>S, CO<sub>2</sub>, acetic acid

### INTRODUCTION

Top of the line corrosion (TLC) was first identified in the sixties<sup>1</sup> and is now a growing concern for the Oil and Gas industry. Many field cases have been published from both onshore and offshore environments<sup>2-7</sup>. This type of corrosion occurs in stratified flow when significant temperature gradients exist between the outside environment and the process fluid, thus leading to water condensation on the internal walls of the pipe line. The presence of this condensed water can induce severe general and pitting corrosion problems, typically on the upper part of the pipe (between 9 and 3 o'clock).

Two main sub-categories of TLC can be identified depending on whether the corrosion mechanism is CO<sub>2</sub> or H<sub>2</sub>S dominated. To be fair, the boundaries delimiting what is a sweet or a sour corrosion are not even clear today but are most likely linked to the type of corrosion product film forming at the metal surface.

---

\* Currently at Lloyd's Register Technical Services Inc.

Top of the line corrosion in sweet conditions has been the focus of intensive research over the past fifteen years and the main corrosion mechanisms involved are now identified, if not well understood. The severity of corrosion attack depends mostly on the condensation rate, the gas temperature, the gas flow rate, the CO<sub>2</sub> partial pressure and the presence of organic acid<sup>13</sup>. Pipe inspections often reveal corrosion over extended areas of the top of the pipeline associated with breakdowns of an otherwise protective FeCO<sub>3</sub> layer. Field experience in this domain is also growing and a lot of research work has been already published<sup>8-12</sup>.

In sour conditions, the mechanism governing top of the line corrosion seems largely different from in sweet conditions. Several pipe failures have been attributed to sour TLC<sup>1,5-7</sup> although the real controlling parameters was often unclear. Limited research work has been published on sour TLC<sup>14-16</sup>, leading often more to interrogation than real answers. Although no firm conclusion can be made at this stage, some important characteristics of sour TLC have been proposed<sup>17</sup>:

- Sour TLC does not seem to be as serious and as common as sweet,
- The condensation rate may not be the main controlling parameter as it is in sweet TLC,
- The severity of the attack seems to depend on the type and protectiveness of the iron sulfide film formed at the condensed water/steel interface,
- Gas temperature consequently, could be a key factor as it directly affects the phase identity and characteristics of the formed iron sulfide.

It is worth noting that the influence of parameters such as temperature, H<sub>2</sub>S partial pressure, or exposure time on the characteristics of the FeS scale formed at the top of the line is the focus of ongoing research. Much more experimental work has been performed on sour bottom of the line corrosion, especially looking at the effect of small amounts of H<sub>2</sub>S<sup>18-21</sup>. The subsequent reduction of the corrosion rate compared to a baseline pure CO<sub>2</sub> environment is associated with the formation of a protective mackinawite film. However, different environmental conditions can lead to the formation of various thermodynamically stable types of FeS<sup>22</sup> and, consequently, various corrosion scenarios. However, the links between the types of FeS formed and their specific corrosion protectiveness have not yet been established.

The presence of organic acids, so aggressive in TLC in a sweet environment<sup>8</sup>, has been reported to greatly affect the protectiveness of mackinawite and lead to localized corrosion at the bottom of the line<sup>23</sup>. There is no reason to believe that the organic acids, condensing together with the water at the top of the line, will not play a key role in the severity of sour TLC.

The objective of this paper is to provide experimental results obtained through a parametric study of the effect of the partial pressures of H<sub>2</sub>S and CO<sub>2</sub> as well as the presence of acetic acid on the top of the line corrosion rate.

The results presented in this paper were obtained through experiments that focused on top of the line and bottom of the line corrosion. The bottom of the line corrosion results are already published elsewhere<sup>23</sup>. References are made to this paper in the following sections and the reader is advised to refer to this previous publication for more details on the experimental procedure and conditions.

## EXPERIMENTAL PROCEDURE

The following sections related to the experimental procedure, focusing on bottom of the line corrosion<sup>23</sup> have already been reported in a conference proceeding of NACE 2007 and in a conference proceeding of NACE 2009 with the sections focusing on CO<sub>2</sub> top of the line corrosion<sup>13</sup>. Consequently, the basic description of the equipment and the procedure has been derived from these two previously published proceedings. Some clarifications have been added to reflect the focus of this paper.

## Experimental Loop

Three different large scale flow loops were used in this study. The experiments were carried out in multiphase stratified flow with water and a mixture of CO<sub>2</sub>/N<sub>2</sub>/H<sub>2</sub>S. The flow loops, made of 316 stainless steel and alloy C276 (for the H<sub>2</sub>S experiments) all have very similar characteristics and they can be divided into three main parts: the tank, the pump and the loop.

- The tank is used for the liquid phase conditioning and heating. It is filled with de-ionized water. Acetic acid is added to reach the concentration requirements of the tests. A set of immersion heaters control the temperature.
- Positive displacement progressive cavity pumps or gas blowers are used to move the liquid or the gas phase.
- The 4" diameter flow loop is 30 meters long and horizontally leveled. The test sections, where the measurements are taken, are located at least 8 meters downstream from the exit of the tank. The test sections (FIGURE 1) are 1.5 meters long pipe spool pieces. Each has up to eight probe ports (four at the top, four at the bottom). In this paper, only the top of the line results are taken into account. Samples of condensed liquid and *in situ* pH measurements were taken at the test section.

The experimental procedure is as follows. The tank is first filled with 1 m<sup>3</sup> of de-ionized water. Carbon dioxide (and nitrogen in some cases) is injected in the loop at a specific pressure. The liquid phase is then heated up to the specific temperature by two electrical resistance heaters. The pump is started and the gas/liquid mixture is directed around the loop in a stratified flow regime. De-oxygenation is performed by depressurizing the mixture several times until the concentration of oxygen is low (<50 ppb). Oxygen concentration is measured using a colorimetric test kit. Once the deoxygenation is complete, acetic acid and/or H<sub>2</sub>S concentrations are adjusted to the required levels. The corrosion probes are then introduced under pressure at the test section and the experiment begins. A data acquisition device is used in order to continuously measure the total pressure and the gas/liquid temperature.

## Liquid Phase Specification

The liquid phase is made up exclusively from deionized water. No salt is added. However, dissolved ferrous iron Fe<sup>2+</sup> build-up occurs throughout the test due to the corrosion process on the weight loss specimens. Data on the evolution of the Fe<sup>2+</sup> concentration and pH during the whole duration of the tests are shown in TABLE 1.

## Acetic Acid Concentration

The acetic acid (HAc) concentration is adjusted by adding a calculated amount of pure HAc (Glacial acetic acid) in the tank. The acetic acid solution is first deoxygenated before being introduced into the tank using a high-pressure vessel connected to the tank. Several liquid samples are then taken and run through an ion chromatograph in order to verify the concentration of total acetate species (free HAc + Ac<sup>-</sup>) introduced in the liquid phase. A differentiation is made between the free or undissociated acetic acid concentration (free HAc) and the total acetic acid concentration which includes all acetate containing species (free HAc and acetate Ac<sup>-</sup>). In order to keep the concentration of free acetic acid constant during the test, the pH of the liquid phase was adjusted (maintained constant) if necessary by adding small amounts of undissociated acetic acid. It should be noted that if the iron concentration increases and the pH is maintained constant by adding HAc the free HAc concentration will change during the exposure.

TABLE 2 presents the calculated free acetic concentration at the bottom of the line for each test.

The concentration of acetic acid was not measured at the top of the line but it has been reported that the concentration of free acetic acid at the bottom of the line should be very similar to the concentration of total acetate species (Free HAc + Ac<sup>-</sup>) in the condensed liquid<sup>12</sup>.

It is important to note that the concentration of free acetic acid injected in the loop is close to the concentration figure measured by ion chromatograph but in most cases a 20-30% discrepancy exists. This discrepancy is most likely the result of the technical difficulties not only often met in large scale loop tests that target a high degree of accuracy in the measurements but also errors possible made in the measurement process. For clarity purposes, the concentration of free acetic acid will be displayed as 100 or 1000 ppm (depending on the test conditions) in this paper.

## Gas Phase Composition

In all the experiments, the gas phase comprised a mixture of CO<sub>2</sub> and N<sub>2</sub> (2 bars of CO<sub>2</sub> and 0.7 bars of N<sub>2</sub>, 0.3 bars of water vapor) for a total pressure of 3 bars. For the H<sub>2</sub>S environment, the required amount of H<sub>2</sub>S was introduced in pure gas form at the beginning of the test and checked regularly using a piston pump and low range standard detection tubes. The trace amounts of H<sub>2</sub>S introduced in the loop were consumed fairly rapidly by the corrosion process and the H<sub>2</sub>S partial pressure had to be adjusted almost every day to maintain an accuracy of ±20%.

## Materials Characterization

All the weight loss specimens are made of API<sup>†</sup> X65 carbon steel prepared from the same piece of field pipe line. The chemical analyses of this X65 steel, its microstructure and its hardness have already been reported elsewhere<sup>23</sup>.

## Condensation Rate Measurement

Vapor phase condensation on the internal pipe wall was achieved by artificially cooling specific segments of the loop (test sections) using coils wrapped around the pipe. Tap water was circulated through the coils and the flow rate was adjusted in order to reach the required amount of cooling. The condensation rate was measured either by using a water trap downstream of the test section or by measuring the difference of temperature between the gas and the pipe wall inner surface. A more detailed presentation of the cooling system is available elsewhere<sup>8,9,13</sup>.

## Localized Corrosion Characterization

Information on the occurrence and extent of localized corrosion was collected for each test performed using a 3D surface profilometer. It is therefore important to define clearly the parameters measured as detailed in the following

Pitting Corrosion: Generally, pits are deep and narrow, and either hemispherical or cup-shaped. When pitting corrosion happens, a part of the material surface undergoes rapid attack while most of the adjacent surface remains unaffected. As described in FIGURE 2, the criteria used to define pitting corrosion are displayed below:

- the pit depth is 5 times bigger than the general corrosion depth ( $b \geq 5a$ ),
- the diameter of pit after film removal is smaller than the pit depth ( $c \leq b$ ).

Mesa Attack: Mesa attack is characterized by a wide and often flat-bottomed local attack without protective corrosion film, surrounded by areas with intact corrosion films. Generally, mesa attack starts as several small pits growing beneath the porous corrosion film. These pits can then continue to grow

---

<sup>†</sup> American Petroleum Institute (API), 1220 L. St. NW, Washington, DC, 20005.

beneath the corrosion film until the lid of the corrosion film is torn away by the mechanical forces of flow. Growth of the pits continues by corrosion both laterally and in depth, then the original corrosion film is removed stepwise by the flow. Several such pits can be initiated during a short period of time and grow together into a wide flat-bottomed mesa attack. A galvanic effect between the film-free corroding metal in the bottom of the mesa attack and the film-covered steel outside the mesa attack can increase the corrosion rate in the mesa attack area. As described in FIGURE 3, the criteria used for mesa attack are:

- the mesa attack depth is 5 times bigger than general corrosion depth ( $b \geq 5a$ ),
- the diameter of mesa is bigger than pit depth ( $c \geq b$ ).

Percentage Of Specimen Surface Affected By Localized Corrosion: Since weight loss steel specimens were used in this study, it was found that the percentage of the specimen surface affected by localized corrosion (pitting and mesa attack together) constituted a likely indication of its occurrence.

### **Corrosion Rate Measurement**

The weight loss specimens were not inserted into the corrosion environment until the system has reached steady state (stable temperature, pressure and flow velocities). The corrosion rates were measured with weight loss specimens made of X65 carbon steel. Samples consisting of circular specimens (0.76 cm internal diameter, 3.17 cm external diameter, and 0.5 cm thickness) with an exposed area of 7.44 cm<sup>2</sup> were polished using isopropanol as a coolant with silicon carbide papers, up to 600 grit. After this preparation, they were covered with liquid polytetrafluoroethylene (PTFE) on the outer edges and bottom. Following four to six hours of curing at ambient conditions, the samples were held at 200°C in an oven for four hours. The uncovered steel surface was then re-polished with 600 grit silicon carbide paper wetted with isopropanol, cleaned, dried and weighed. A picture of a specimen after preparation is shown in FIGURE 4. The specimens were then flush mounted on the internal pipe wall of the loop by using a specially designed probe holder, which meant that only one face of the specimen was in direct contact with the corrosive environment. The exposure time was between 2 and 21 days in all experiments. Upon removal from the loop, the specimen surface was flushed with isopropanol, to dehydrate it; photographs of the surface were then taken. The weight of the specimen after each test was registered, and the ASTM<sup>‡</sup> G1 standard procedure was followed to remove the corrosion products and determined the corrosion rate by weight loss. One specimen is generally used for weight loss, and the other is preserved for corrosion product evaluation by scanning electron microscopy (SEM) and energy dispersion analysis (EDS).

### **Test Matrix**

TABLE 3 presents the experimental conditions of each test. Only two parameters (free acetic acid concentration and H<sub>2</sub>S partial pressure) were varied around a set of baseline conditions (Test 1). The influence of these two parameters were studied separately (Test 2 to 6) and then combined in Test 7, 8 and 9. More information about the test conditions has been already reported<sup>23</sup>.

The nine experiments conducted to investigate different aspects of the corrosion process in a CO<sub>2</sub> environment can be divided into three groups:

- Influence of the concentration of free acetic acid;
- Influence of the partial pressure of H<sub>2</sub>S;
- Combined effect of the concentration of free acetic acid and the partial pressure of H<sub>2</sub>S.

---

<sup>‡</sup> ASTM International, 100 Barr Harbor Drive, West Conshohocken, PA 19428.

Apart from the acetic acid concentration and the partial pressure of H<sub>2</sub>S, all the other experimental parameters were kept at a fixed values (system temperature: 70°C, partial pressure of CO<sub>2</sub>: 2 bars, total pressure: 3 bars, gas velocity: 5 m/s).

## RESULTS

The corrosion results related to the effect of acetic acid on CO<sub>2</sub> dominated TLC also, results on pure sour TLC have already been presented in previous NACE conference proceedings<sup>13,14,23</sup>.

### Corrosion Rate Results

The corrosion rate results are displayed in a series of plots from FIGURE 5 to FIGURE 14. In addition to the evolution of the average (uniform) corrosion rate with time, key data about the occurrence of localized corrosion are displayed. The graphs present corrosion rates due to pitting or mesa attack and they also indicate the percentage of surface area of the specimen affected by localized corrosion (pitting or mesa). The corresponding values were obtained by performing a surface analysis on each specimen with a 3D surface profilometer. The average (uniform) corrosion rate was calculated using the weight loss of a specimen and the time of exposure. Error bars representing the maximum and minimum values and the number of specimens (number of repeated measurements) are displayed where applicable on each graph.

#### Influence Of The Free Acetic Acid Concentration.

The influence of the concentration of free acetic acid on the corrosion rate at the top of the line is shown in FIGURE 5 and FIGURE 6. The effect of 100 ppm of free acetic acid seems mild, but 1000 ppm almost doubles the corrosion rate. In addition, while pure CO<sub>2</sub> TLC rates tend to decrease rapidly with time due to the formation of a protective FeCO<sub>3</sub> layer, the corrosion rate with 1000 ppm of acetic acid remains almost constant at 2 mm/year after 3 weeks of testing. Moreover, the presence of acetic acid strongly promotes the occurrence of pitting corrosion (pitting rate was 7.5 mm/year after 3 weeks of testing), this is proportional to the amount of acid in the solution. The continuous renewal of condensed droplets made more corrosive by the presence of acid acetic vapor is believed to be responsible for the breakdown of corrosion product layer protectiveness.

#### Influence Of The Partial Pressure Of Hydrogen Sulfide.

FIGURE 7 and FIGURE 8 present information about general and localized corrosion in environments containing H<sub>2</sub>S but no acetic acid. The presence of trace amounts of H<sub>2</sub>S (pH<sub>2</sub>S=0.04 bar, CO<sub>2</sub>/H<sub>2</sub>S ratio: 500) clearly decrease the corrosion rate compared to a pure CO<sub>2</sub> environment. This is generally explained by the formation of a very protective film of iron sulfide on the surface of the metal. It is expected that further addition of H<sub>2</sub>S (pH<sub>2</sub>S up to 0.13 bar, CO<sub>2</sub>/H<sub>2</sub>S ratio: 15) should cause a gradual increase in the corrosion rate. This is not obviously the case at the top of the line where it is difficult to identify a distinct trend. The additional cathodic reaction may compete with an increase in protectiveness of the iron sulfide film. It seems however, that the corrosion decreases rapidly in the first 15 days and then reverses this tendency and increases slightly. One of the main differences with a pure CO<sub>2</sub> environment is that the corrosion process does not seem to slow down considerably, even if the severity of the attack is lower. No localized corrosion (pitting or mesa attack) was observed at the top of the line in the conditions tested.

#### Combined Effect Of The Acetic Acid And The Hydrogen Sulfide.

The influence of acetic acid on H<sub>2</sub>S TLC is shown in FIGURE 9 to FIGURE 14. As in a CO<sub>2</sub>/H<sub>2</sub>S environments, the TLC rates remained more or less constant during the entire duration of the test. While 100 ppm of free acetic acid seems to have little effect, the corrosion rate jumps from 0.3 to 1.8 mm/year with 0.004 bar of H<sub>2</sub>S when 1000 ppm of the weak acid is present. It is interesting to note that,

with traces of H<sub>2</sub>S (pH<sub>2</sub>S=0.004 bar, CO<sub>2</sub>/H<sub>2</sub>S ratio: 500), the average top of the line corrosion rate after 21 days of exposure is similar to the one obtained in pure CO<sub>2</sub> environment when a significant amount of free acetic acid is present (FIGURE 13). Further increases in H<sub>2</sub>S partial pressure (0.13 bar of H<sub>2</sub>S, CO<sub>2</sub>/H<sub>2</sub>S ratio: 15) seem to reverse this tendency and offer better protection against top of the line corrosion. The average corrosion rate after 3 weeks of exposure is still three to four times higher with 1000 ppm of acetic acid than without.

In the presence of acetic acid, some localized corrosion was observed but only in the form of small pits. The percentage area affected by pitting corrosion is usually very limited (unlike in a pure CO<sub>2</sub> environment) and pitting rates do not exceed 4 mm/year, which barely qualifies the corrosion as pitting in accordance with what was learned in the procedure presented earlier.

## **Surface Analysis**

The corrosion product layer for each test was systematically studied using SEM, EDS and 3D surface profilometer. However, the complete characterization of corrosion product films (and especially the multiple possible phases of iron sulfide films) requires XRD analysis, in this study, was not performed owing to issues with equipment availability and conflict with project deadlines. Therefore, even if the visual observations obtained by SEM give some useful indications about the nature of the corrosion product film, some caution should be taken when interpreting these observations.

### Influence Of The Free Acetic Acid Concentration.

The surface analysis associated with the influence of acetic acid on CO<sub>2</sub> top of the line corrosion is shown in FIGURE 15 and FIGURE 16. A protective FeCO<sub>3</sub> film usually forms at the metal surface when supersaturation conditions are reached in the droplet of condensed water (high pH, associated with high Fe<sup>2+</sup> concentration). The presence of high concentrations of free acetic acid (1000 ppm of free acetic acid at the bottom of the line) clearly affects the relative protectiveness of the scale by decreasing the pH of the freshly condensed liquid (local acidification leading to some FeCO<sub>3</sub> dissolution) and by adding another cathodic reaction. Numerous breakdowns of the layer are seen all over the specimen surface. Localized corrosion occurs through pitting and mesa attacks.

### Influence Of The Partial Pressure Of Hydrogen Sulfide.

SEM and EDS analysis of the corrosion layer formed in CO<sub>2</sub>/H<sub>2</sub>S environments without acetic acid are shown in FIGURE 17 (pH<sub>2</sub>S= 0.004 bar, CO<sub>2</sub>/H<sub>2</sub>S ratio: 500) and FIGURE 18 (pH<sub>2</sub>S= 0.13 bar, CO<sub>2</sub>/H<sub>2</sub>S ratio: 15). In all case, even though the tests were performed with 2 bars of CO<sub>2</sub>, no FeCO<sub>3</sub> crystals could be clearly identified (although their presence cannot be ruled out). Instead, a mostly macroscopically amorphous corrosion product layer covers the specimen surface. The layer does not always appear to be homogeneous, especially at higher H<sub>2</sub>S partial pressures where large parts of the product layer seem to have peeled off during the corrosion process. In addition, peculiar features (which show obvious crystalline structure) could be observed but could not be clearly identified as EDS analysis always shows similar peaks of iron (Fe) and sulfide (S). In all cases, the steel was uniformly corroded and no localized corrosion could be observed even after 21 days of exposure to the corrosive environment.

### Combined Effect Of Acetic Acid And Hydrogen Sulfide.

The surface analysis associated with the influence of acetic acid on CO<sub>2</sub>/H<sub>2</sub>S top of the line corrosion is shown in FIGURE 19 to FIGURE 21. The corrosion product layer at the top of the line is made of FeS as it is usually the case at the top of the line in H<sub>2</sub>S environments. In all cases, the film looks fairly uniform, quite porous and easily wiped off the surface of the specimen. The film is also, in most cases, cracked; this cracking is believed to take place over time owing to internal mechanical stress. The corrosion process could then continue under the film. FeCO<sub>3</sub> crystals could be observed in these

cracks. There is no clear difference in the EDS analysis (identification of the film composition) performed for the tests with or without acetic acid. The surface looks evenly corroded except for a few isolated pits, especially at higher contents of acetic acid. Once again, the extent of localized corrosion seems to be very mild with maximum pitting rates being usually close to average corrosion rates.

## CONCLUSIONS

Influence of the acetic acid concentration on CO<sub>2</sub> Top of the Line Corrosion

- The presence of acetic acid increases the initial corrosion rate at the top of the line.
- In a CO<sub>2</sub> environment, the presence of significant concentrations of acetic acid strongly promotes localized corrosion. The effect seems to be proportional to the amount of acid present.

Main characteristics of H<sub>2</sub>S/CO<sub>2</sub> Top of the Line Corrosion

- In the presence of H<sub>2</sub>S, the average corrosion rate at the top and the bottom of the line starts at a low value and remains relatively constant over time.
- The presence of traces of H<sub>2</sub>S retards the average corrosion rate compared to a pure CO<sub>2</sub> environment. There is no clear influence of further additions of H<sub>2</sub>S (up to 0.13 bar) on the average corrosion rate.
- At the top of the line, no localized corrosion was observed in the presence of H<sub>2</sub>S (up to 0.13 bar) after 21 days of testing.

Influence of the presence of acetic acid on CO<sub>2</sub>/H<sub>2</sub>S Top of the Line Corrosion

- In the presence of H<sub>2</sub>S, the presence of acetic acid seems to affect the integrity of the FeS film and also strongly influences the general corrosion rate.
- The presence of acetic acid in sour conditions seems to trigger the occurrence of localized corrosion in the form of small pits. The maximum pitting rate measured is, however, falls close to the average corrosion rate and therefore is of fairly low intensity.

## ACKNOWLEDGEMENTS

The authors would like to express their gratitude to Total, BP, ConocoPhillips, Chevron, Occidental Oil Company, Saudi Aramco and ENI for the financial support of this research and for allowing the publication of this paper. The authors are also grateful for the contributions of Dezra Hinkson, Ziru Zhang and Dr. Victor Wang, colleagues at the Institute, to this experimental work. Finally, the authors are thankful to Dr. David Young for his guidance and expertise on sulfide chemistry and H<sub>2</sub>S corrosion phenomena.

**TABLE 1:**  
Experimental conditions

	Acetic acid series						H <sub>2</sub> S series						Acetic acid/H <sub>2</sub> S series					
	Test 1		Test 2		Test 3		Test 4		Test 5		Test 6		Test 7		Test 8		Test 9	
Duration	pH	Fe <sup>2+</sup> ppm	pH	Fe <sup>2+</sup> ppm	pH	Fe <sup>2+</sup> ppm	pH	Fe <sup>2+</sup> ppm	pH	Fe <sup>2+</sup> ppm	pH	Fe <sup>2+</sup> ppm	pH	Fe <sup>2+</sup> ppm	pH	Fe <sup>2+</sup> ppm	pH	Fe <sup>2+</sup> ppm
At start	NA	NA	3.4	N/A	N/A	N/A	4.2	7.9	4.3	9	4.4	6.5	4.8	40	4.4	56.3	3.9	76
After 2 days	4.6	0.4	N/A	N/A	3.9	70	4.4	19	4.4	N/A	4	25	N/A	N/A	4.2	145	4.3	94
After 7 days	4.9	8.4	N/A	10	3.6	40	4.4	19	4.5	N/A	4.1	23	4.7	N/A	4.5	110	4.3	N/A
After 14 days	4.6	11	4	24	3.7	36	4.6	N/A	4.4	18	4.3	25	4.7	70	4.5	150	4.1	170
After 21 days	4.8	11	4	17	3.7	32	4.7	18	4.5	20	4.3	26	4.7	35	4.6	170	4.3	140

**Notes :**

pH and Fe<sup>2+</sup> measurements are taken from the bulk liquid phase in the tank – They do not represent the chemistry in the condensed liquid

N/A: Not available

**TABLE 2: Acetic acid concentration**

Test #	Measured total acetate species ([free HAc] + [Ac <sup>-</sup> ]) in the liquid phase with ion chromatograph (ppm)	Calculated free acetic acid concentration in the liquid phase at the bottom of the line (ppm)	
		based on the amount of acetate species measured with ion chromatography	based on the amount of acetate species introduced in the experimental loop
Test 2	57	Between 50 and 55	Between 87 and 96
Test 3	675	Between 605 and 664	Between 895 and 944
Test 7	N/A	N/A	Between 46 and 57
Test 8	1052	Between 656 and 846	Between 630 and 810
Test 9	1120	Between 861 and 1002	Between 772 and 895

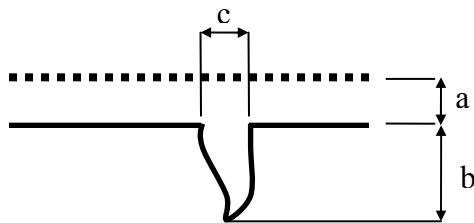
**TABLE 3: Test matrix**

Common parameters:  
 Steel type: X65  
 Liquid phase composition: DI water  
 Test duration: 3 weeks  
 Absolute pressure: 3 bars  
 pCO<sub>2</sub>: 2 bars  
 Gas temperature: 70 °C  
 Gas velocity: 5 m/s  
 Superficial liquid velocity < 0.05 m/s

Experiment #	1	2	3	4	5	6	7	8	9
Investigating	Acetic acid			H <sub>2</sub> S			Acetic acid / H <sub>2</sub> S		
Free HAc tank (ppm)	0	100	1000	0	0	0	100	1000	1000
pH <sub>2</sub> S (bar)	0	0	0	0.004	0.07	0.13	0.004	0.004	0.13

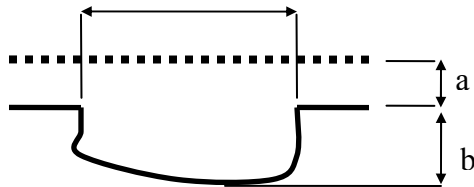


**FIGURE 1:** Test section of the H<sub>2</sub>S loop



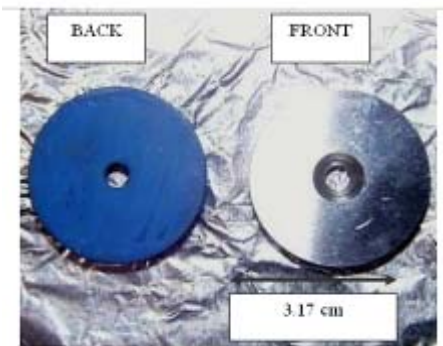
a: general corrosion depth  
 b: pit depth after film removal  
 c: diameter of pit after film removal

**FIGURE 2:** Schematic representation of pitting corrosion



a: general corrosion depth  
 b: pit depth after film removal  
 c: diameter of pit after film removal

**FIGURE 3:** Schematic representation of mesa attack



Weight loss specimens (Teflon coating at the back and the side)



Specimen holder configuration

**FIGURE 4:** Weight loss specimens with Teflon coating at the back and the side (External diameter = 3.17 cm)

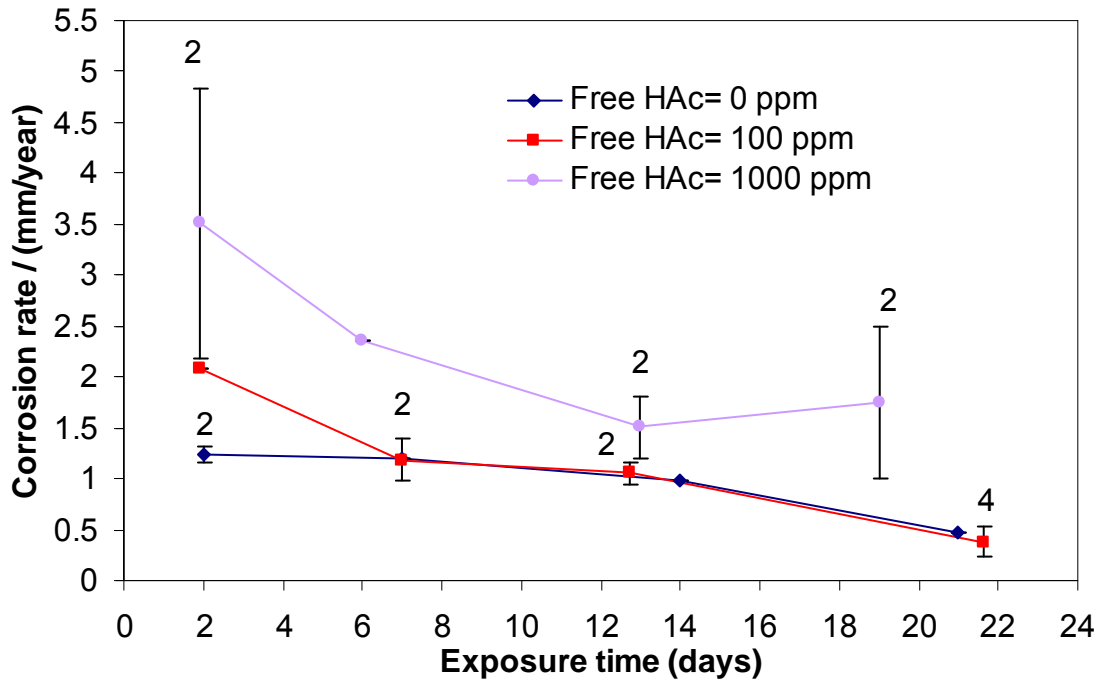


**FIGURE 5:** Influence of the free HAc concentration  
Evolution of the general corrosion rate over time  
( $P_T$ : 3 bars,  $p_{CO_2}$ : 2 bars,  $p_{H_2S}$ : 0 bar,  $T_g$ : 70°C,  $V_g$ : 5 m/s)

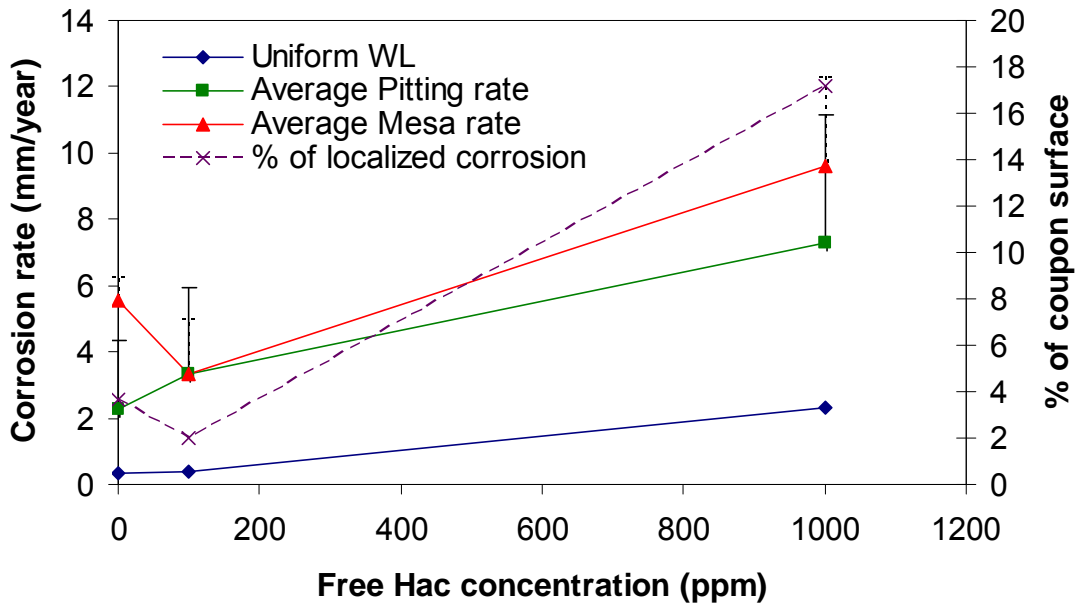


**FIGURE 6:** Localized corrosion – Influence of the free HAc concentration in pure CO<sub>2</sub> environment  
Evolution of the general corrosion rate over time  
( $P_T$ : 3 bars,  $p_{CO_2}$ : 2 bars,  $p_{H_2S}$ : 0 bar,  $T_g$ : 70°C,  $V_g$ : 5 m/s, Exposure time: 21 days)

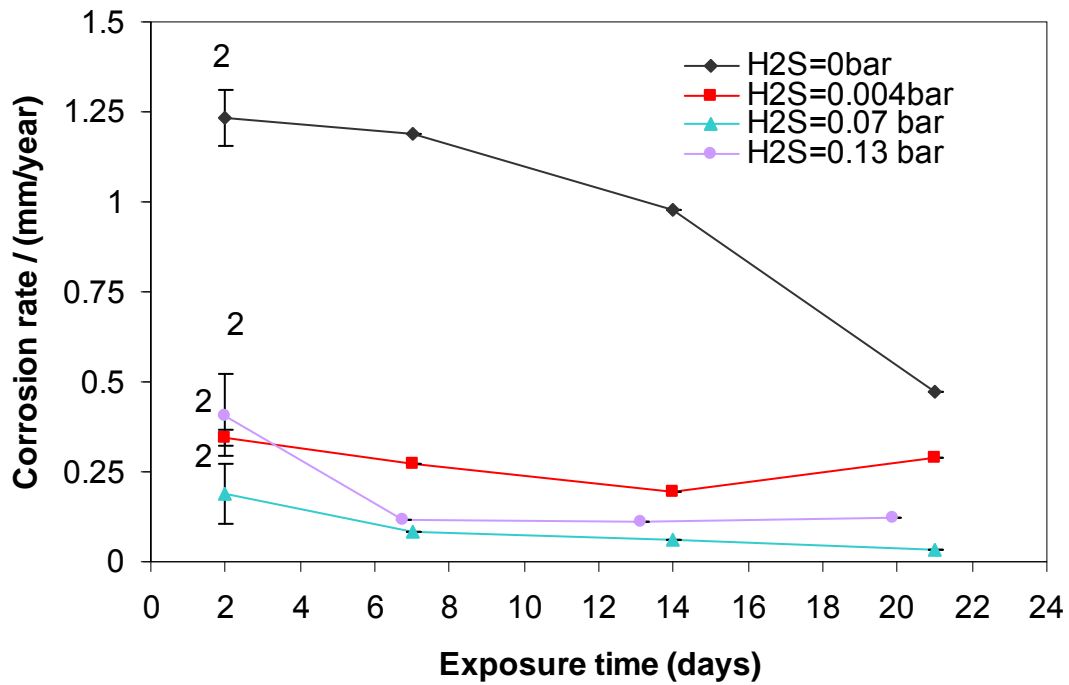


**FIGURE 7:** Influence of the partial pressure of H<sub>2</sub>S  
 Evolution of the general corrosion rate with the partial pressure of H<sub>2</sub>S  
 (P<sub>T</sub>: 3 bars, pCO<sub>2</sub>: 2 bars, Free HAc: 0 ppm, T<sub>g</sub>: 70°C, V<sub>g</sub>: 5 m/s)

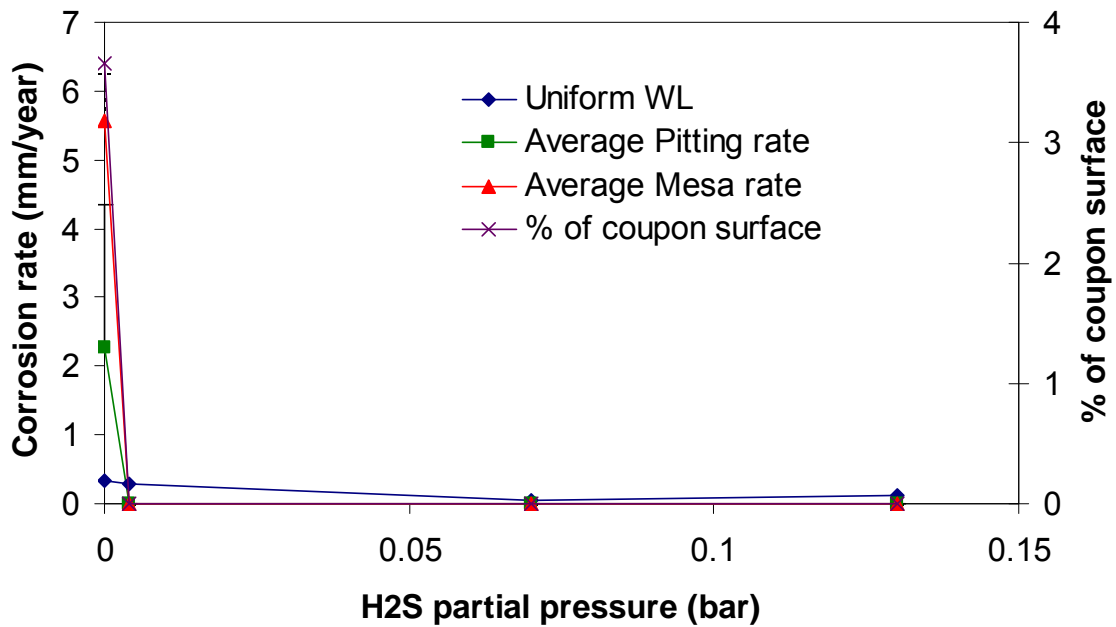


**FIGURE 8:** Localized corrosion – Influence of the H<sub>2</sub>S partial pressure  
 (P<sub>T</sub>: 3 bars, pCO<sub>2</sub>: 2 bars, Free HAc: 0 ppm, T<sub>g</sub>: 70°C, V<sub>g</sub>: 5 m/s, Exposure time: 3 weeks)

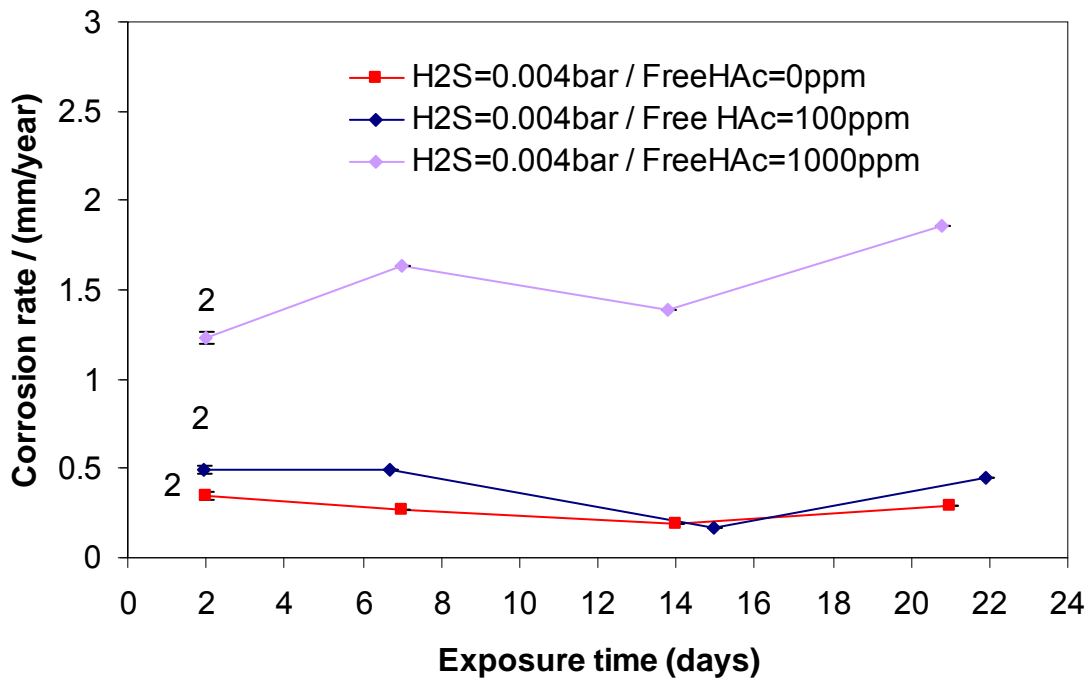


**FIGURE 9:** Combined effect of the partial pressure of H<sub>2</sub>S and the concentration of free HAc  
Evolution of the general corrosion rate over time  
(P<sub>T</sub>: 3 bars, pCO<sub>2</sub>: 2 bars, pH<sub>2</sub>S: 0.004 bar, T<sub>g</sub>: 70°C, V<sub>g</sub>: 5 m/s)

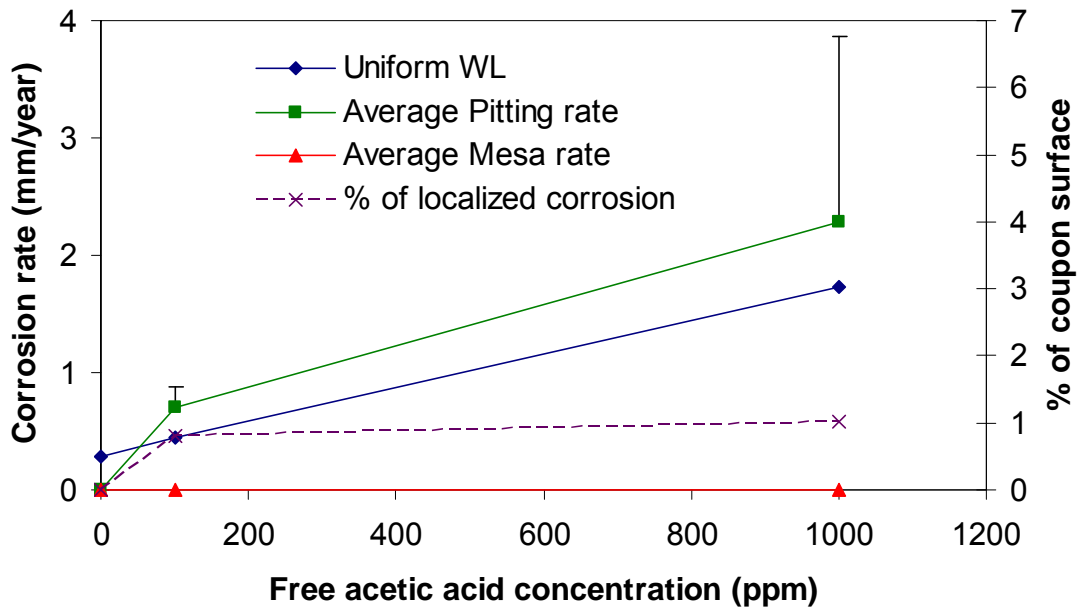


**FIGURE 10:** Localized corrosion – Influence of the free HAc concentration in CO<sub>2</sub>/H<sub>2</sub>S environment  
(P<sub>T</sub>: 3 bars, pCO<sub>2</sub>: 2 bars, pH<sub>2</sub>S: 0.004 bar, T<sub>g</sub>: 70°C, V<sub>g</sub>: 5 m/s, Exposure time: 3 weeks)

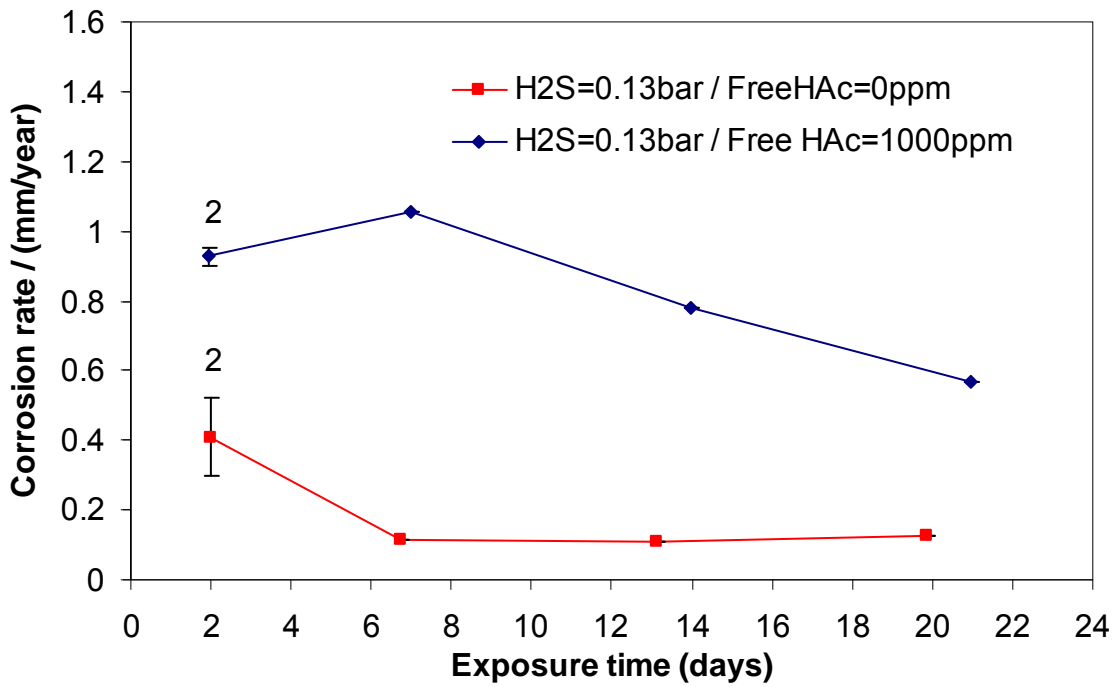


**FIGURE 11:** Combined effect of the partial pressure of H<sub>2</sub>S and the concentration of free HAc  
Evolution of the general corrosion rate over time  
(P<sub>T</sub>: 3 bars, pCO<sub>2</sub>: 2 bars, pH<sub>2</sub>S: 0.13 bar, T<sub>g</sub>: 70°C, V<sub>g</sub>: 5 m/s)

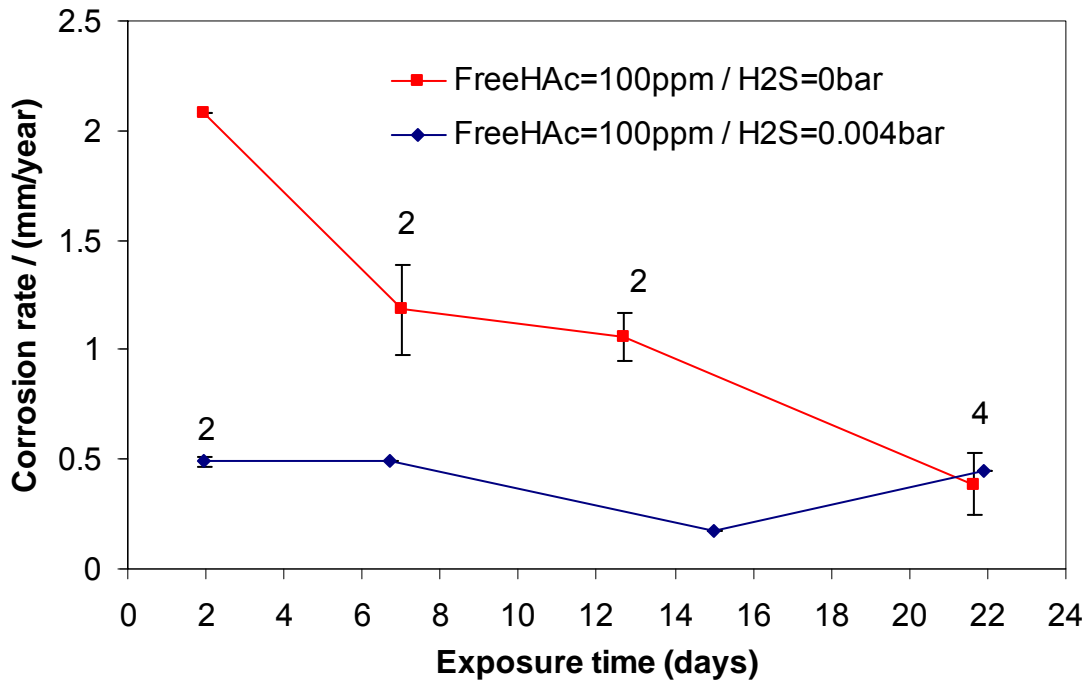


**FIGURE 12:** Combined effect of the partial pressure of H<sub>2</sub>S and the concentration of free HAc  
Evolution of the general corrosion rate over time  
(P<sub>T</sub>: 3 bars, pCO<sub>2</sub>: 2 bars, Free HAc: 100 ppm, T<sub>g</sub>: 70°C, V<sub>g</sub>: 5 m/s)

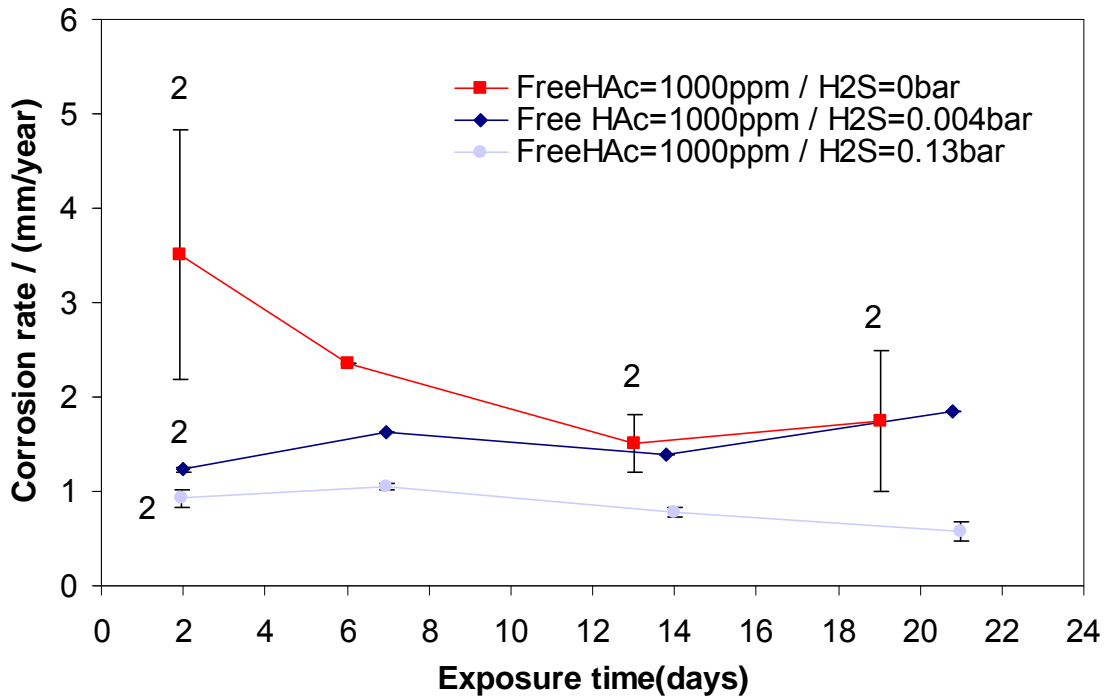


**FIGURE 13:** Combined effect of the partial pressure of H<sub>2</sub>S and the concentration of free HAc  
Evolution of the general corrosion rate over time  
(P<sub>T</sub>: 3 bars, pCO<sub>2</sub>: 2 bars, Free HAc: 1000 ppm, T<sub>g</sub>: 70°C, V<sub>g</sub>: 5 m/s)

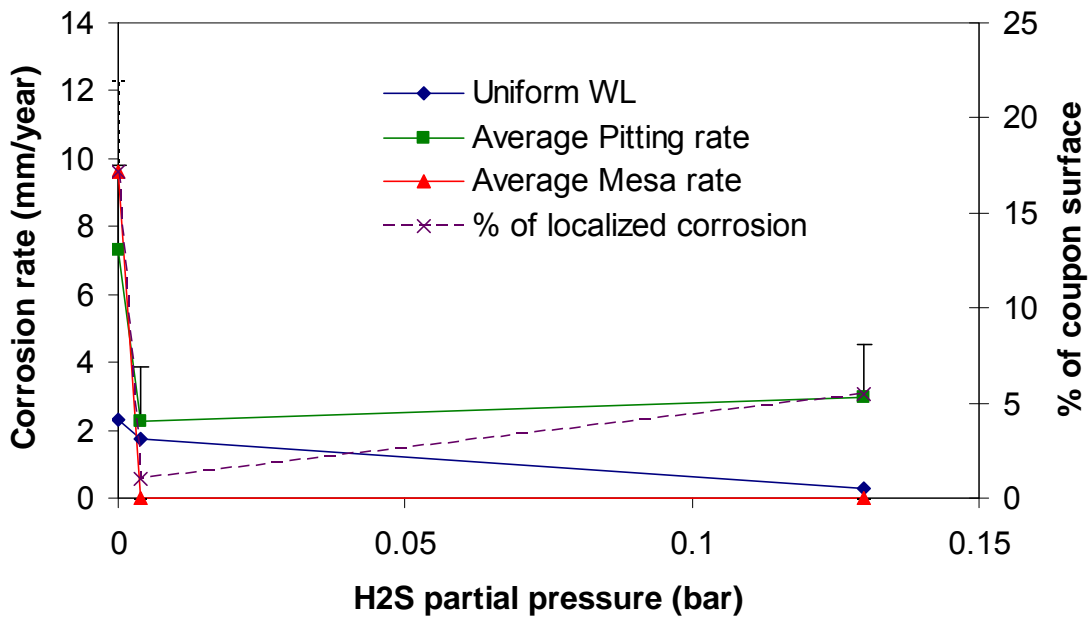


**FIGURE 14:** Localized corrosion – Influence of the free HAc concentration in CO<sub>2</sub>/H<sub>2</sub>S environment  
(P<sub>T</sub>: 3 bars, pCO<sub>2</sub>: 2 bars, Free HAc: 1000ppm, T<sub>g</sub>: 70°C, V<sub>g</sub>: 5 m/s, Exposure time: 3 weeks)

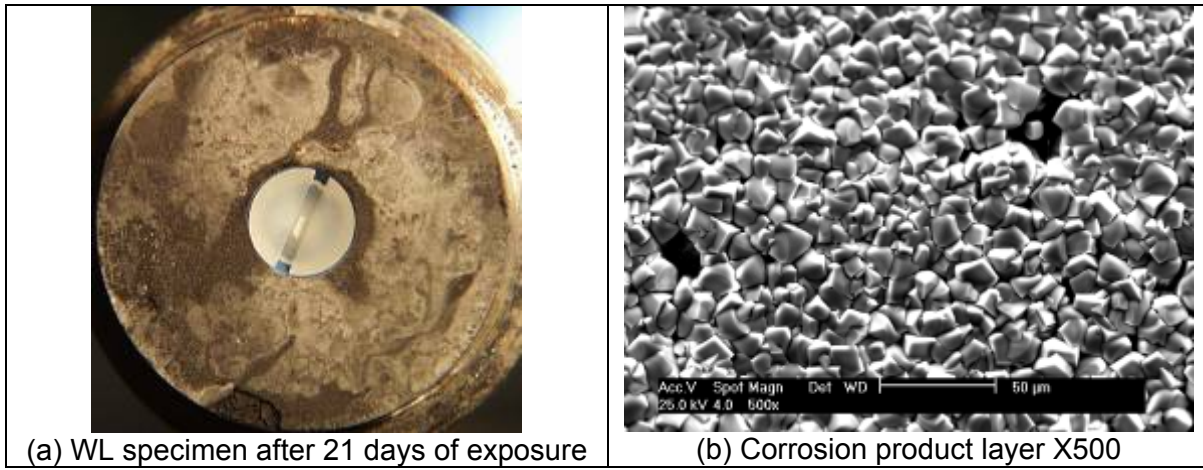


**FIGURE 15:** Test 1 – Pure CO<sub>2</sub> environment  
 (pCO<sub>2</sub>: 2 bars, pH<sub>2</sub>S: 0 bar, Free HAc: 0 ppm, T<sub>g</sub>: 70°C, V<sub>g</sub>: 5 m/s, Exposure time: 3 weeks)

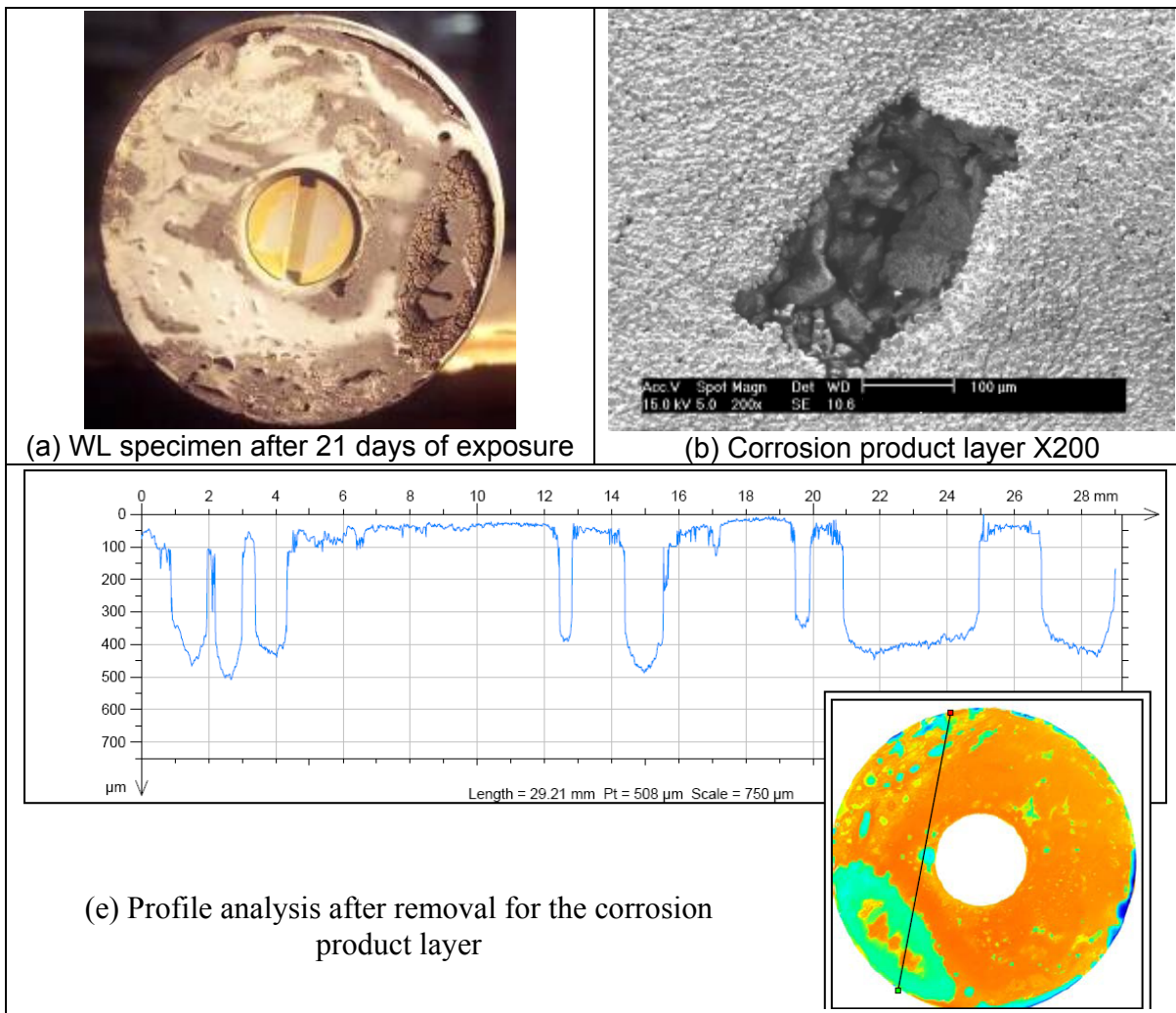


**FIGURE 16:** Test 3 – Pure CO<sub>2</sub> environment with acetic acid  
 (pCO<sub>2</sub>: 2 bars, pH<sub>2</sub>S: 0 bar, Free HAc: 1000 ppm, T<sub>g</sub>: 70°C, V<sub>g</sub>: 5 m/s, Exposure time: 3 weeks)

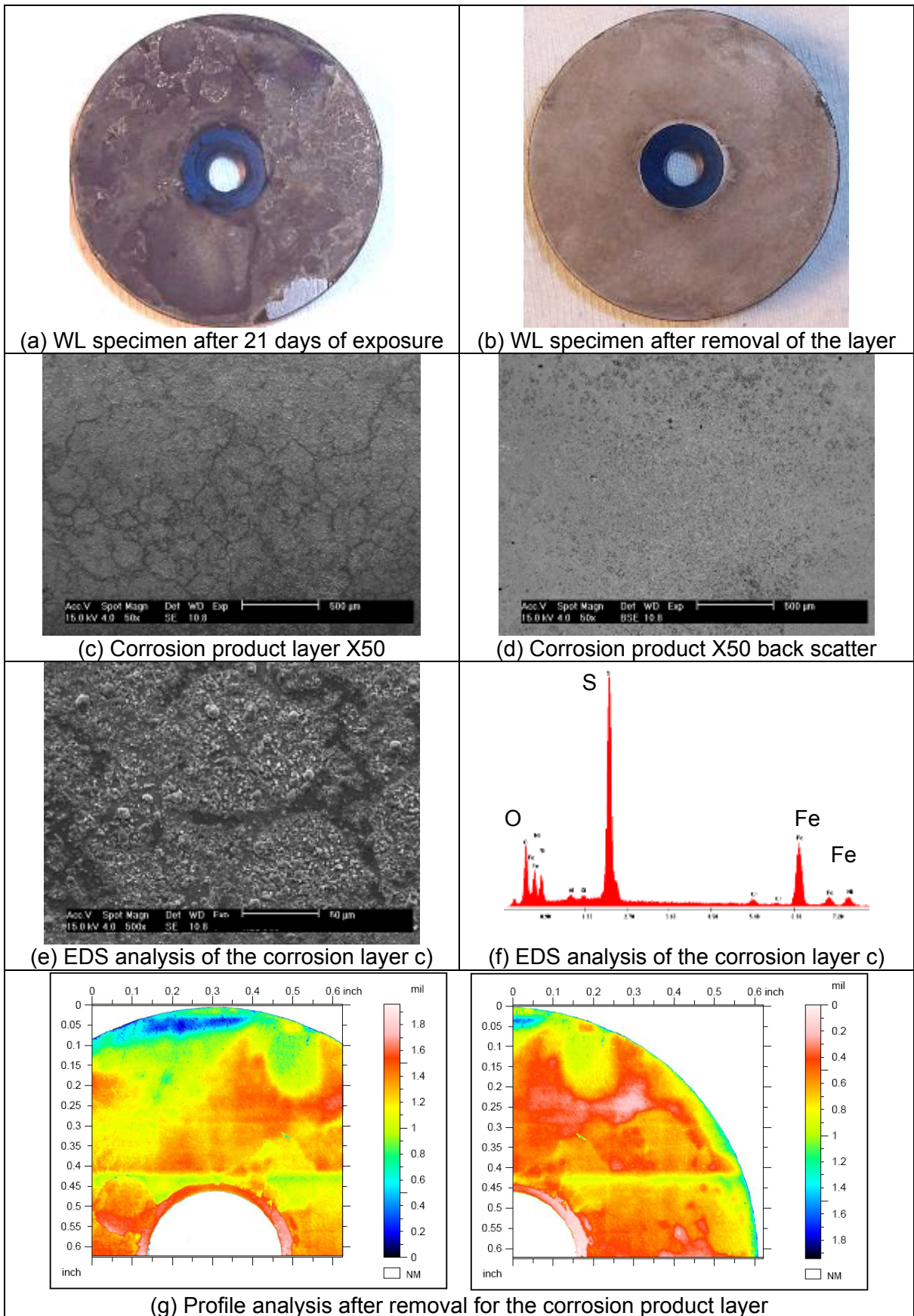


**FIGURE 17:** Test 4 – CO<sub>2</sub> environment with traces of H<sub>2</sub>S – CO<sub>2</sub>/H<sub>2</sub>S: 500 (pCO<sub>2</sub>: 2 bars, pH<sub>2</sub>S: 0.004 bar, Free HAc: 0 ppm, T<sub>g</sub>: 70°C, V<sub>g</sub>: 5 m/s, Exposure time: 3 weeks)

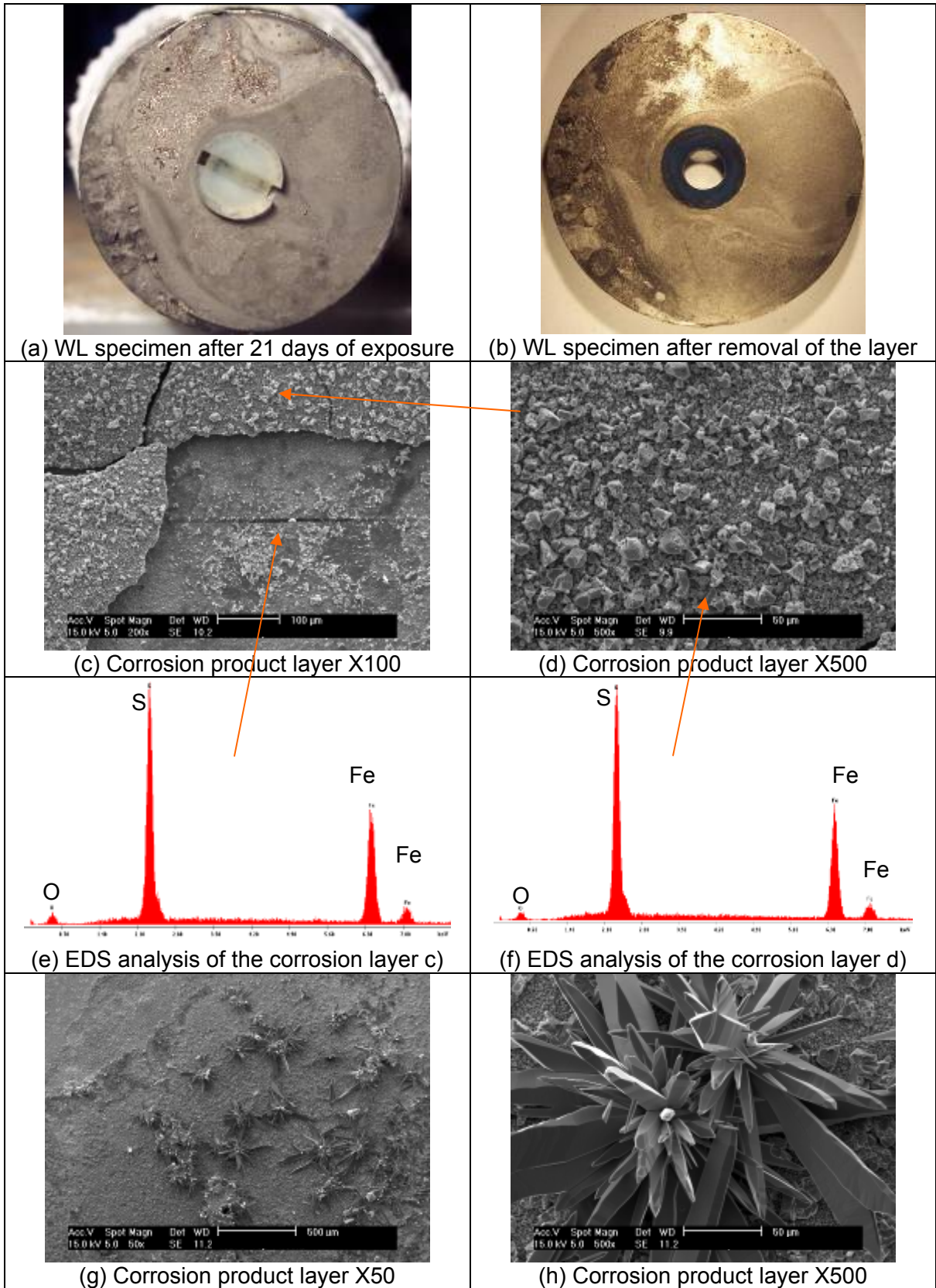


**FIGURE 18:** Test 6 – CO<sub>2</sub> environment with H<sub>2</sub>S – CO<sub>2</sub>/H<sub>2</sub>S: 15  
 (pCO<sub>2</sub>: 2 bars, pH<sub>2</sub>S: 0.13 bar, Free HAc: 0 ppm, T<sub>g</sub>: 70°C, V<sub>g</sub>: 5 m/s, Exposure time: 3 weeks)

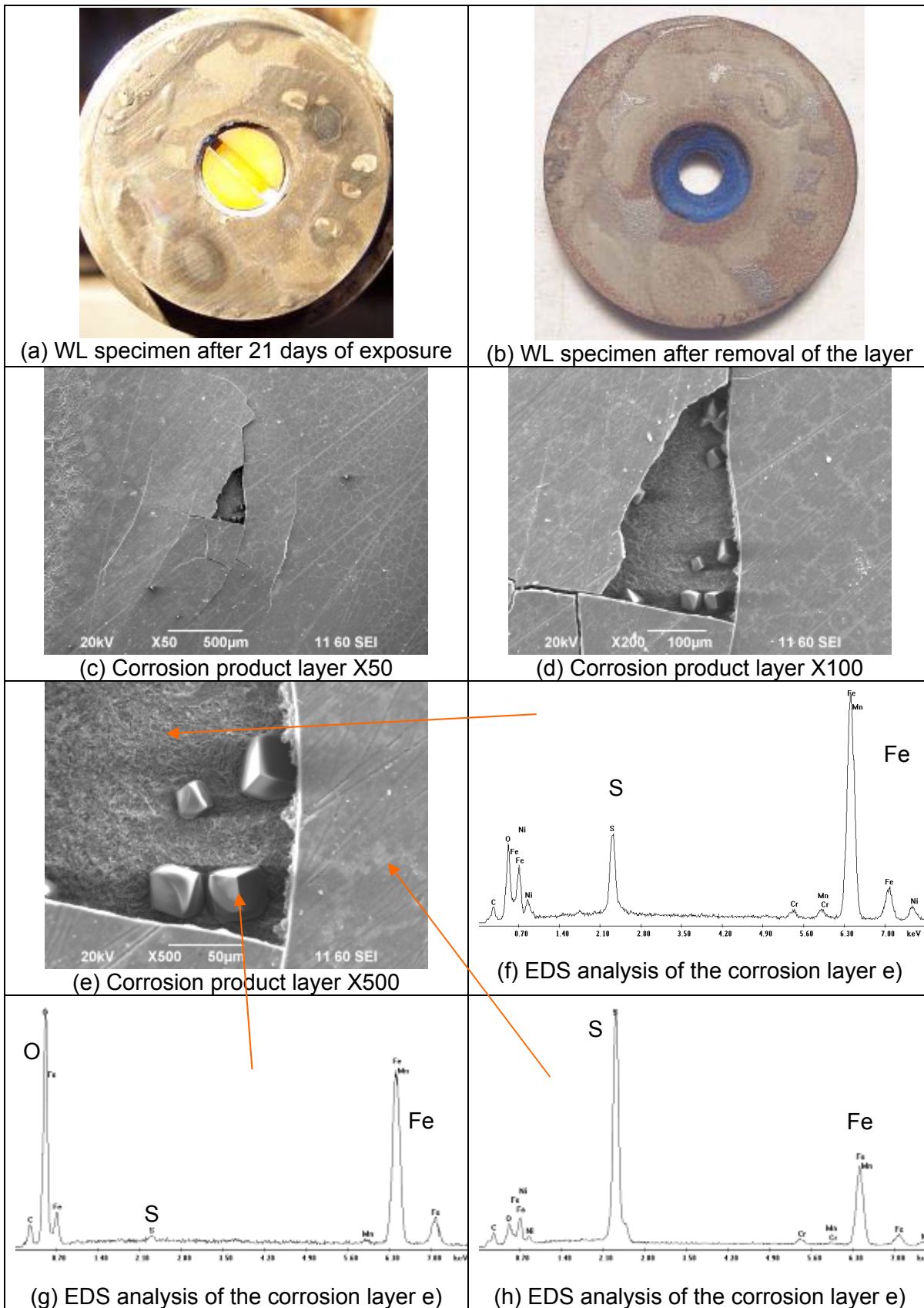


**FIGURE 19:** Test 7 – CO<sub>2</sub> environment with traces of H<sub>2</sub>S and acetic acid – CO<sub>2</sub>/H<sub>2</sub>S: 500 (pCO<sub>2</sub>: 2 bars, pH<sub>2</sub>S: 0.004 bar, Free HAC: 100 ppm, T<sub>g</sub>: 70°C, V<sub>g</sub>: 5 m/s, Exposure time: 3 weeks)

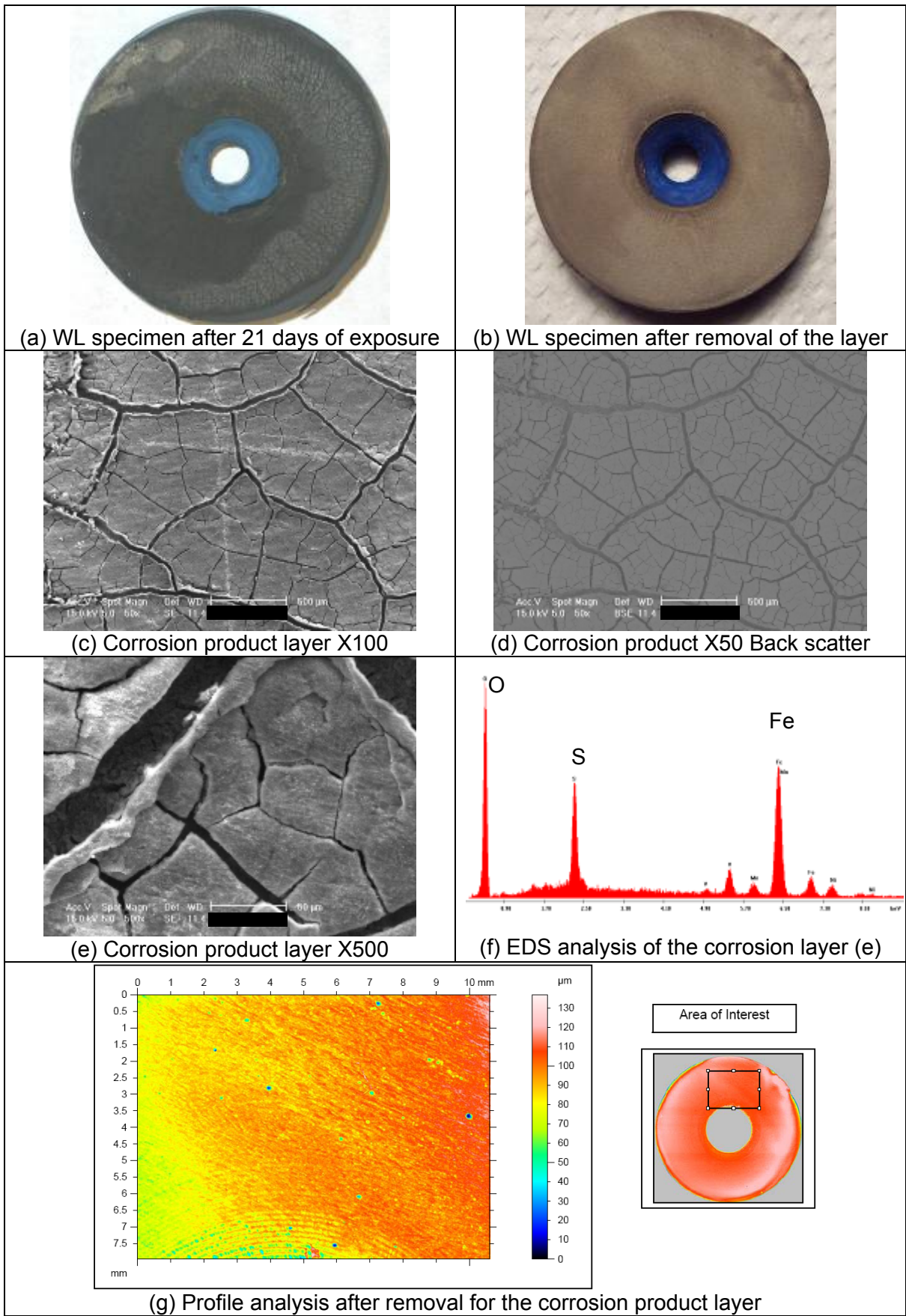


**FIGURE 20:** Test 8 – CO<sub>2</sub> environment with traces of H<sub>2</sub>S and acetic acid – CO<sub>2</sub>/H<sub>2</sub>S: 500 (pCO<sub>2</sub>: 2 bars, pH<sub>2</sub>S: 0.004 bar, Free HAC: 1000 ppm, T<sub>g</sub>: 70°C, V<sub>g</sub>: 5 m/s, Exposure time: 3 weeks)

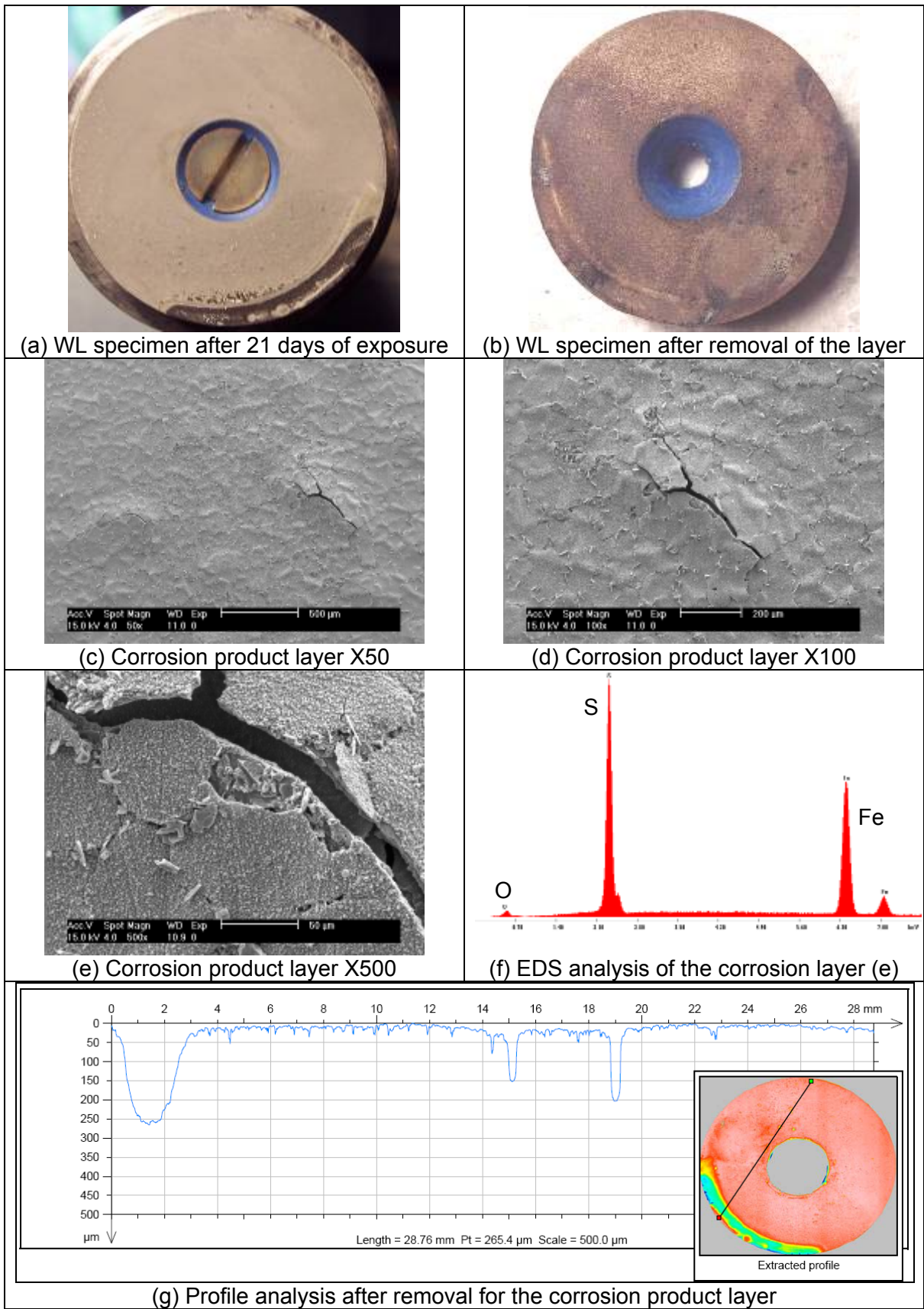


**FIGURE 21:** Test 9 – CO<sub>2</sub> environment with H<sub>2</sub>S and acetic acid – CO<sub>2</sub>/H<sub>2</sub>S: 15 (pCO<sub>2</sub>: 2 bars, pH<sub>2</sub>S: 0.13 bar, Free HAc: 1000 ppm, T<sub>g</sub>: 70°C, V<sub>g</sub>: 5 m/s, Exposure time: 3 weeks)

## REFERENCES

1. Paillassa R., Dieumegard M., Estevoyer M., "Corrosion control in the gathering system at Lacq sour gas field", 2<sup>nd</sup> Intl. Congress of Metallic Corrosion, NACE, pp 410-417, New York, 1963.
2. Gunaltun Y.M., Supriyataman D., Jumakludin A., "Top of the line corrosion in multiphase gas line. A case history", Corrosion 99, paper 36 (Houston, TX: NACE International, 1999).
3. Thammachart M., Gunaltun Y., Punpruk S., "The use of inspection results for the evaluation of batch treatment efficiency and the remaining life of the pipelines subjected to top of line corrosion", Corrosion 08, paper 8471 (New Orleans, LA: NACE International 2008).
4. Gunaltun Y., Larrey D., "Correlation of cases of top of the line corrosion with calculated water condensation rates", Corrosion 00, paper 71 (Houston, TX: NACE International, 2000).
5. Ho-Chung-qui D.F., Williamson A.I., Eng P., "Corrosion experiences and inhibition practices in wet sour gathering systems", Corrosion 87, Paper 46 (San Francisco, CA: NACE International, 1987).
6. Edwards M., Cramer B., "Top of the line corrosion –Diagnostic, root cause analysis and treatment", Corrosion 00, Paper 72 (Houston, TX: NACE International, 2000)
7. Martin R.L., "Control of Top-of-line Corrosion in Sour Gas Gathering Pipeline with Corrosion Inhibitors", Corrosion 09, Paper 9288 (Atlanta, GA: NACE International, 2009).
8. M. Singer, S. Nestic, Y. Gunaltun, "Top of the line corrosion in presence of acetic acid and carbon dioxide", Corrosion 04, paper 4377 (Houston, TX: NACE International, 2004).
9. C. Mendez, M. Singer, A. Camacho, S. Hernandez, S. Nestic, "Effect of acetic acid, pH and MEG on the CO<sub>2</sub> top of the line corrosion", Corrosion 05, paper 5278 (Houston, TX: NACE International, 2005).
10. Andersen T., Halvorsen A.M.K., A. Valle A., Kojen G., Dugstad A., "The influence of condensation rate and acetic acid concentration on TOL corrosion in multiphase pipelines", Corrosion 07, paper 7312 (Nashville TN, NACE International 2007).
11. Nyborg R., Dugstad A., "Top of the line corrosion and water condensation rates in wet gas pipelines", Corrosion 07, paper 7555 (Nashville TN, NACE International 2007).
12. Hinkson D., Singer M., Zhang Z., Nestic S., "A study of the chemical composition and corrosivity of the condensate in top of the line corrosion", Corrosion 08, paper 8466 (New Orleans, LA: NACE International 2008).
13. Singer M., Nestic S., Hinkson D., Zhang Z., Wang H., "CO<sub>2</sub> top of the line corrosion in presence of acetic acid - A parametric study", Corrosion 09, paper 9292 (Atlanta, GA: NACE International, 2009).
14. Camacho A., Singer M., Brown B., Nestic S., "Top of the Line Corrosion in H<sub>2</sub>S/CO<sub>2</sub> Environments", Corrosion/08, paper# 8470 (New Orleans, LA: NACE International 2008).
15. Nyborg R., Dugstad A., Martin T., "Top of Line Corrosion with High CO<sub>2</sub> and Traces of H<sub>2</sub>S", Corrosion 09, Paper 9283 (Atlanta, GA: NACE International, 2009).
16. Pugh D.V. et al, "Top-of-Line Corrosion Mechanism for Sour Wet Gas Pipelines", Corrosion 09, Paper 9285 (Atlanta, GA: NACE International, 2009).
17. Bonis, M, "Form sweet to sour TLC: what's different?", Second International TLC Conference, Bangkok, 2009.
18. A. Valdes, R. Case, M. Ramirez, A. Ruiz, "The effect of small amounts of H<sub>2</sub>S on CO<sub>2</sub> corrosion of carbon steel," Corrosion 98, paper 22 (Houston, TX: NACE International, 1998).
19. J. Kvarekval, "The influence of small amounts of H<sub>2</sub>S on CO<sub>2</sub> corrosion of iron and carbon steel," Eurocorr 97, Trondheim, Norway.

20. B. Brown, K.L. Lee, S. Nestic, "Corrosion in multiphase flow containing small amounts of H<sub>2</sub>S", Corrosion 03, paper 3341 (Houston, TX: NACE International, 2003).
21. B. Brown, S. Reddy Parakala, S. Nestic, "CO<sub>2</sub> corrosion in presence of trace amounts of H<sub>2</sub>S", Corrosion 03, paper 4736 (Houston, TX: NACE International, 2004).
22. S. Smith, M. Joosten, "Corrosion of carbon steel by H<sub>2</sub>S in CO<sub>2</sub> containing environments", Corrosion 06, paper 6115 (Houston, TX: NACE International, 2006).
23. Singer M., Brown B., Camacho A., Nestic S., "Combined effect of CO<sub>2</sub>, H<sub>2</sub>S and acetic acid on bottom of the line corrosion", Corrosion/07, paper# 7661 (Nashville TN, NACE International 2007).